Esterification synthesis of iron oxide nanoparticle tracers for magnetic particle imaging (MPI)

Ambar C. Velazquez-Albino[1], Bianca Elsea[1], Andrii Melnyk[1], Neel Eswaran[2], Eric D. Imhoff[1], Aleia G. Williams[3], Willem Graham,[3] Jacqueline Anne Johnson[3], Charles E. Johnson[3], Megan M. Butala[2], and Carlos M. Rinaldi-Ramos[1,4,*]

[1]Department of Chemical Engineering, University of Florida, Gainesville, FL 32611, USA

[2]Department of Materials Science and Engineering, University of Florida, Gainesville, FL 32611, USA

[3]Department of Mechanical, Aerospace and Biomedical Engineering, University of Tennessee Space Institute, Tullahoma, TN 37388, USA

[4]J. Crayton Pruitt Department of Biomedical Engineering, University of Florida, Gainesville, FL 32611, USA

Supporting Information

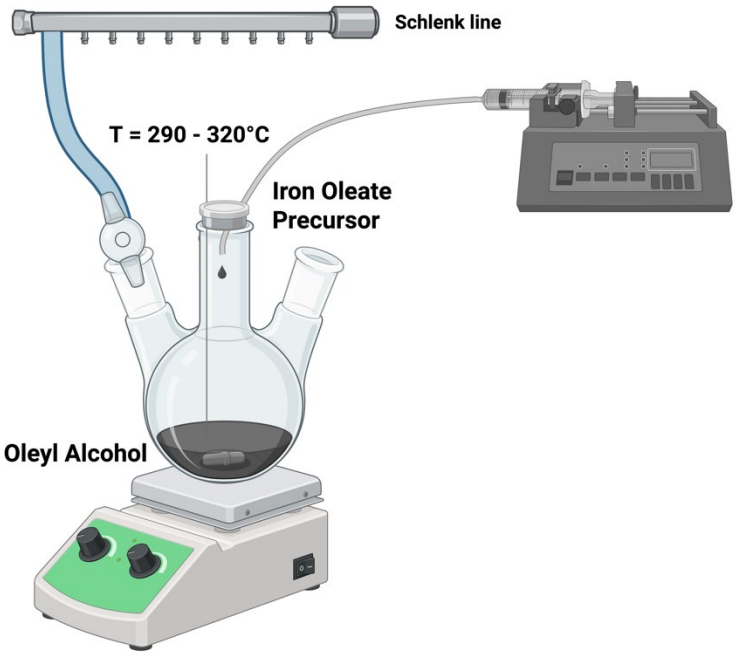

Scheme S1. Experimental setup for esterification synthesis of iron oxide nanoparticles.

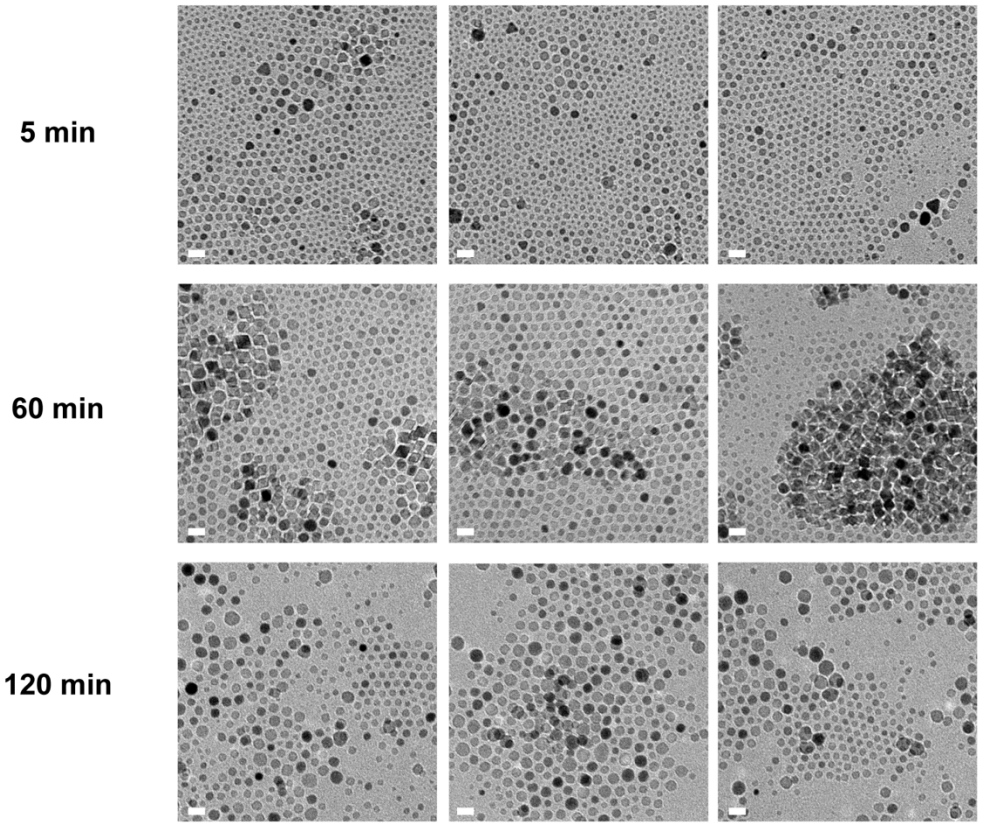

Figure S1. Additional transmission electron microscopy (TEM) images for low temperature esterification synthesis of iron oxide nanoparticles at 290°C and a precursor addition rate of 0.1 mmol/min. Scale bars are 20 nm.

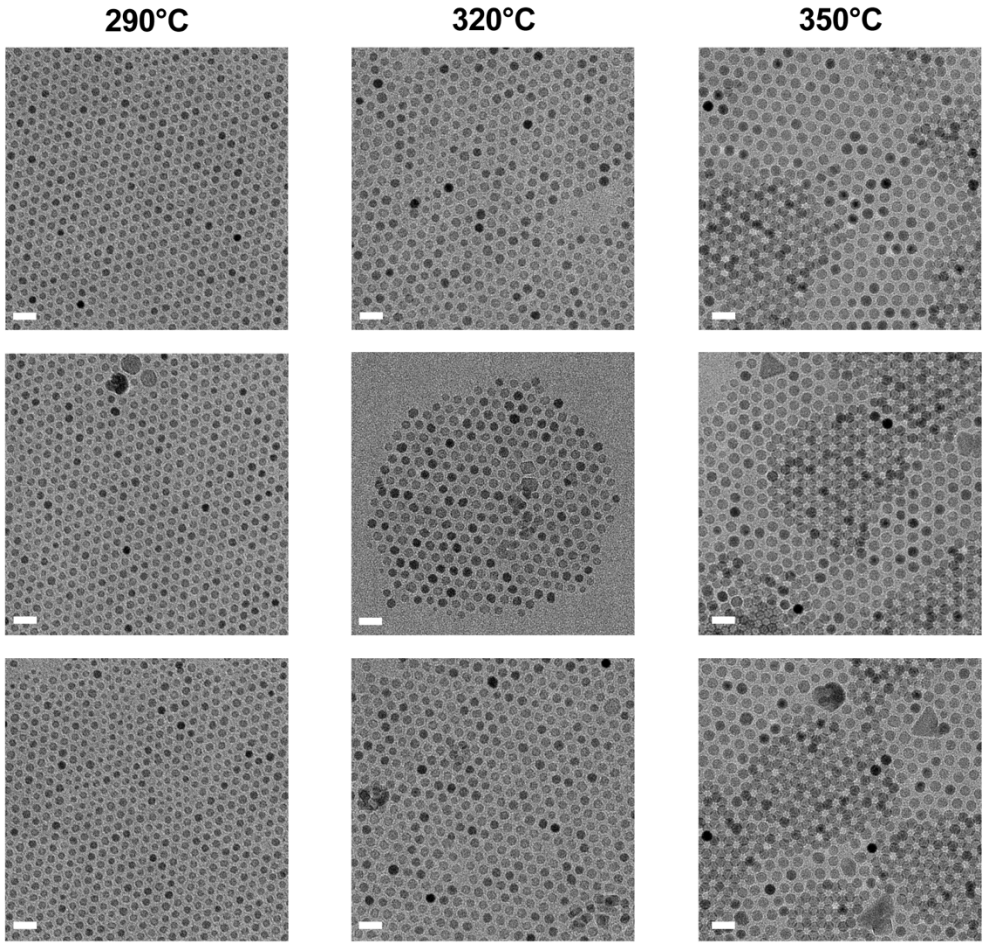

Figure S2. Representative TEM images for esterification reaction temperature study. Scale bars are 20 nm.

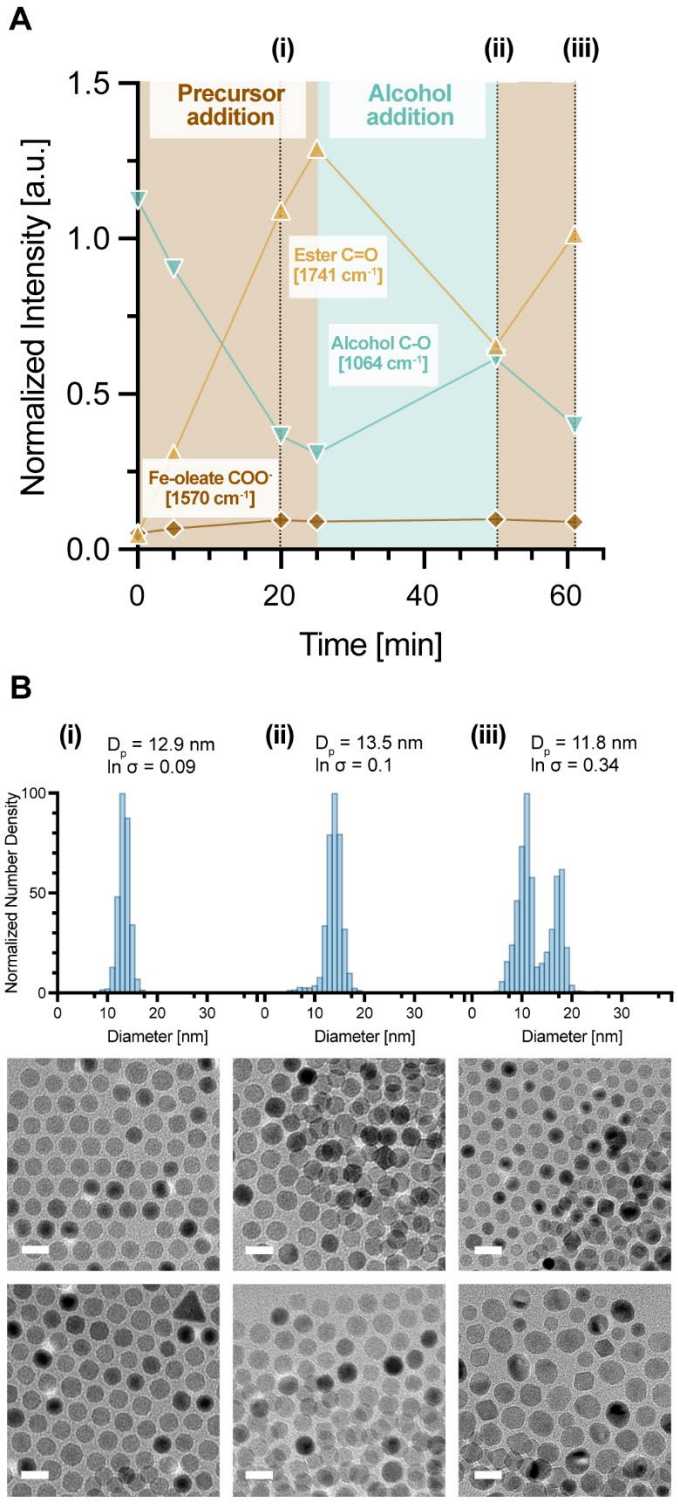

Figure S3. Longer synthesis at 350 °C and a precursor addition rate of 0.05 mmol$_{Fe}$/min is limited due to fast oleyl alcohol boiloff. (A) Trends in FTIR peaks suggests the reaction runs out of oleyl alcohol at around 25 min of Fe-oleate precursor addition (brown), stalling the esterification reaction and nanoparticle growth. Oleyl alcohol was slowly replenished in the reactor (teal) and a condenser was added to slow down alcohol evaporation during the second precursor addition

(brown). (B) Physical size distribution obtained from analysis of TEM images of nanoparticles obtained for aliquots denoted as (i), (ii), and (iii) show that particle growth significantly slows down when precursor is stalled during the alcohol addition stage (teal). After the secondary precursor addition stage, the product obtained (iii) shows a bimodal population of particles, with a high geometric deviation (geometric deviation, ln σ_p) when analyzed as a lognormal distribution to compare polydispersity. Scale bars are 20 nm.

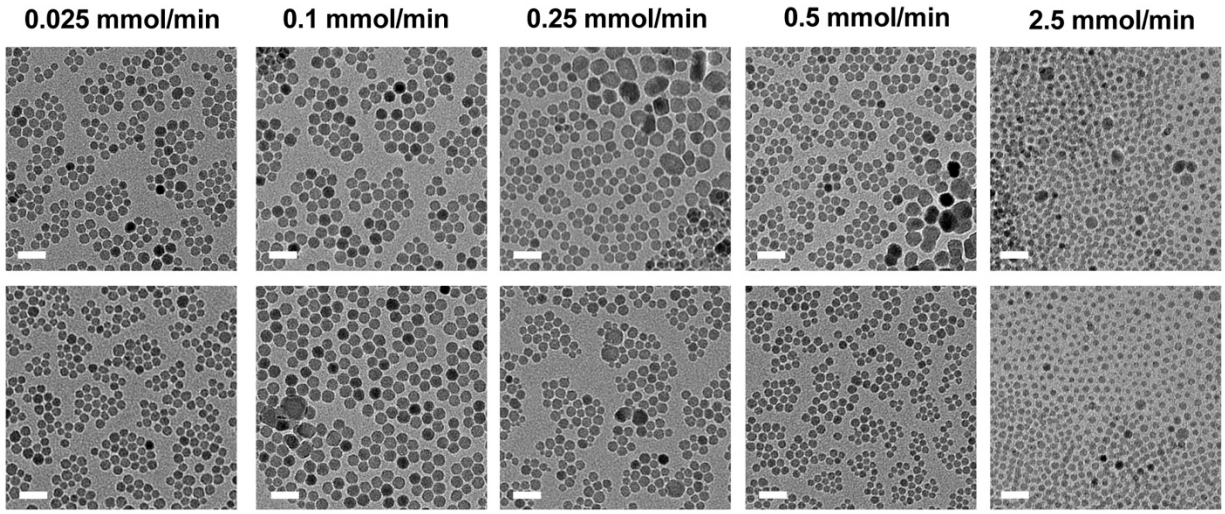

Figure S4. Representative TEM images of nanoparticles synthesized by addition of 1 mmol of Fe at various flow rates at 320°C compared in Figure 2B. Scale bars are 20 nm.

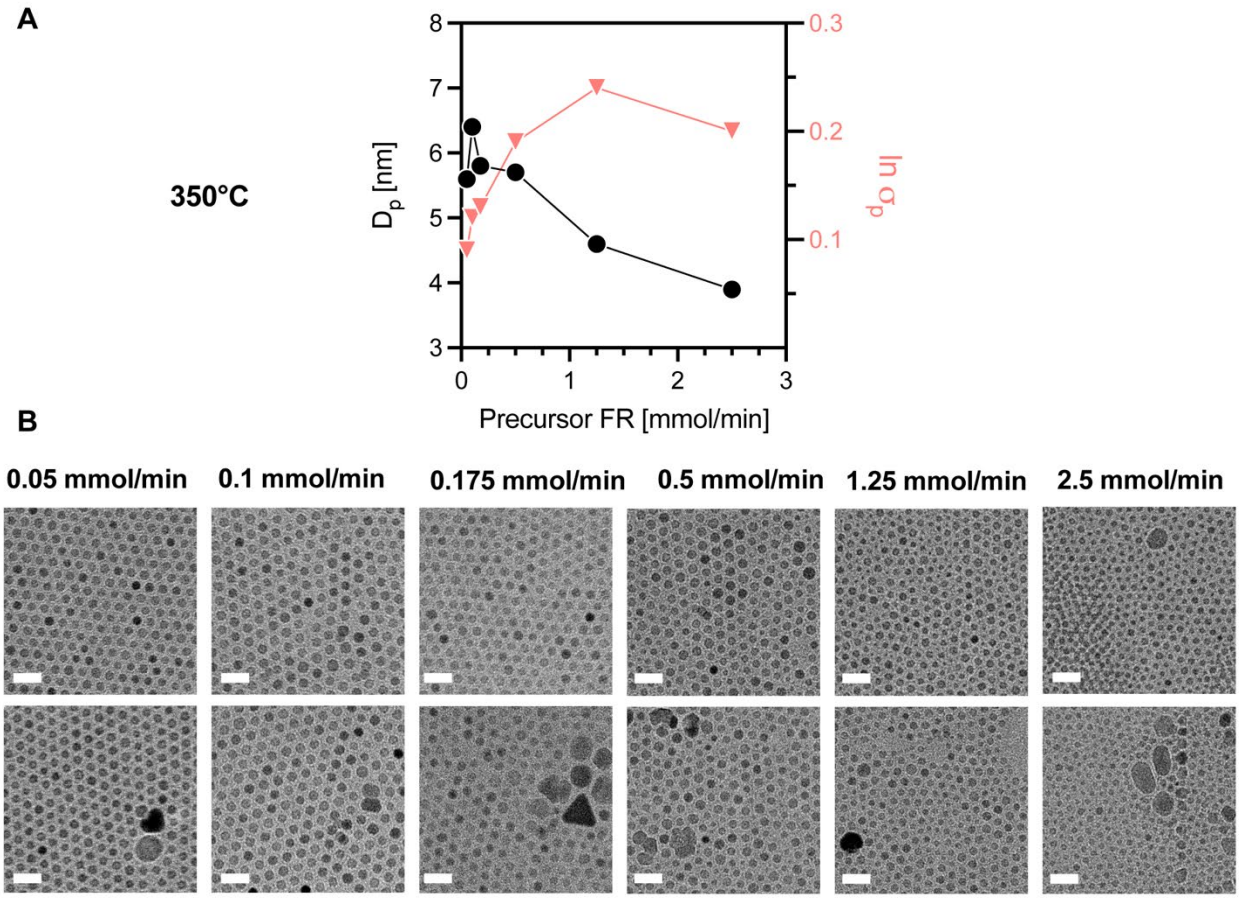

Figure S5. Effect of flow rate on nanoparticle physical size and polydispersity at 350 °C. (A) Results with addition of 1 mmol Fe show that lower flow rates result in larger nanoparticles with a more uniform size distribution (geometric deviation, ln σ_p). (B) Representative TEM images of nanoparticle samples compared for this study. Scale bars are 20 nm.

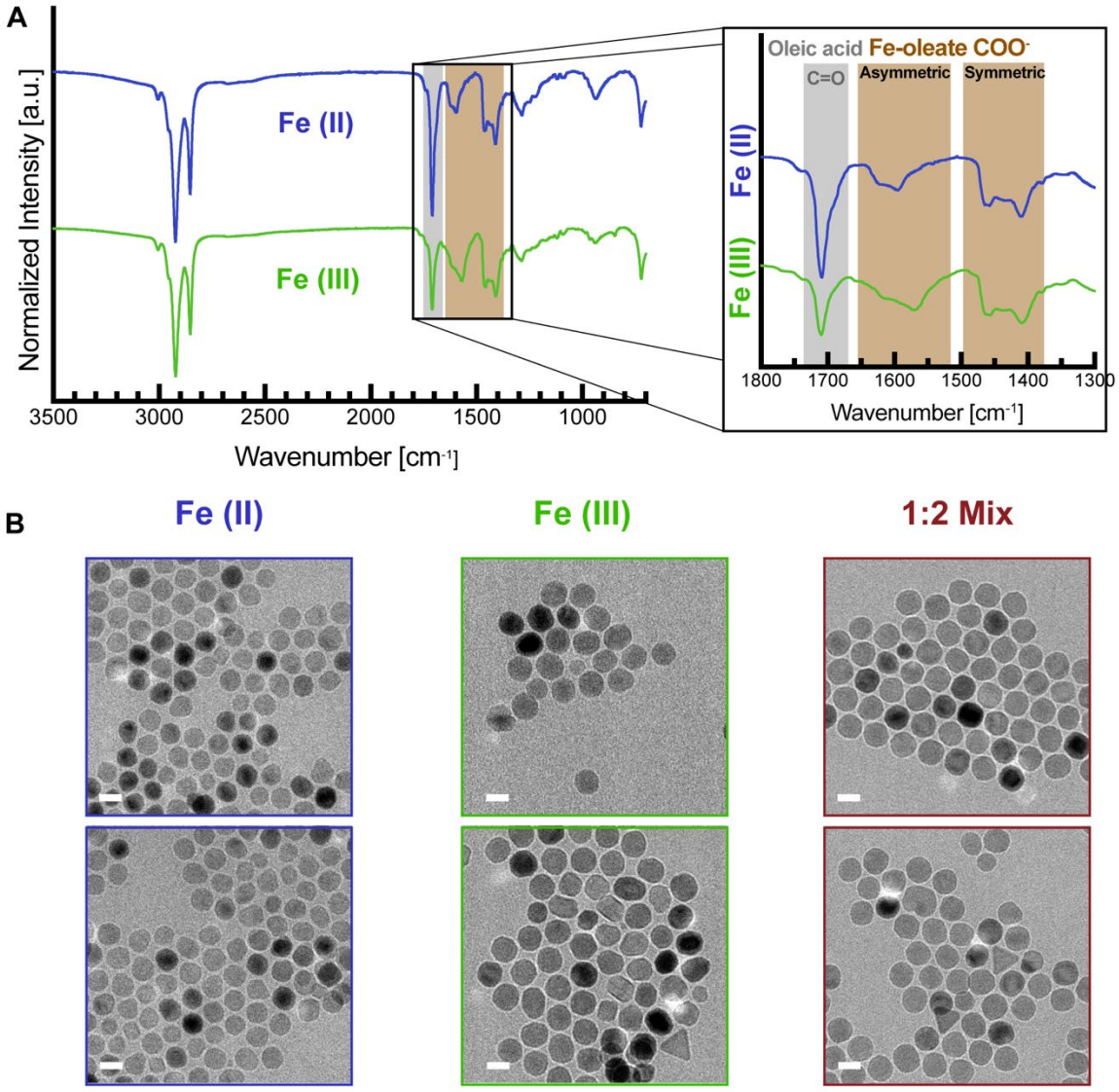

Figure S6. (A) FTIR spectra of Fe (II) and Fe (III) oleates synthesized using $Fe(ac)_2$ and $Fe(acac)_3$, respectively. The Fe (II) oleate commonly used in the esterification literature is synthesized at 150 °C for 1 hour with an oleic acid:metal ratio of 6.3. The Fe (III) oleate used comparison is the precursor used in our previous thermal decomposition work, synthesized ramping to 325 °C with a well-defined FTIR spectra and an oleic acid:metal ratio of 5. (B) Additional TEM images of iron oxide nanoparticles synthesized at 320 °C and 0.1 mmol/min with the Fe (II) oleate, Fe (II) oleate, and the 1:2 Mix (based on bulk magnetite).

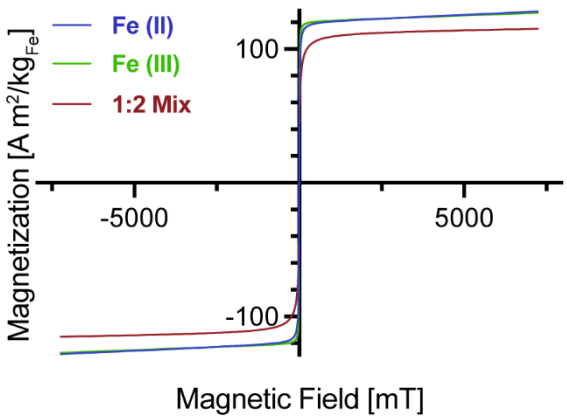

Figure S7. Magnetization versus magnetic field curve at room temperature under a DC magnetic field shows superparamagnetic behavior and similar saturation magnetization for Fe (II) and Fe (III) samples, close to that of bulk magnetite (120 A m^2/kg_{Fe}).

Table S1. Mössbauer spectroscopy hyperfine fitting parameters measured at 293 K. Magnetic hyperfine field (B_{hf}), isomer shift (δ), quadrupole splitting (ΔE_q), full-width-at-half-maximum (Γ). Estimated errors are in B_{hf} ±0.5 T, δ±0.03 mm/s, ΔE_q±0.04 mm/s, in Γ ±0.01, and relative area ±3%.

Sample	Fit Site (Spectra Color)	B_{hf} (T)	δ (mm/s)	ΔE_q (mm/s)	Γ (mm/s)	Relative area (%)	Attribution
Fe (II)	Site1 (Teal)	46.8	0.28	-0.01	0.60	33	Magnetite A (tetrahedral) site Fe^{3+} and Maghemite A & B sites Fe^{3+}
	Site 2 (Pink)	42.4	0.57	-0.01	0.76	58	Magnetite B (octahedral) site $Fe^{2.5+}$ (valence averaged)
	Site 3 (Orange)	0.0	0.81	0.63	0.55	9	Wüstite ($Fe_{1-x}O$) Fe^{2+} site
Fe (III)	Site 1 (Teal)	47.7	0.30	-0.01	0.51	58	Magnetite A (tetrahedral) site Fe^{3+} and Maghemite A & B sites Fe^{3+}
	Site 2 (Pink)	43.4	0.56	0.00	0.85	42	Magnetite B (octahedral) site $Fe^{2.5+}$ (valence averaged)
1:2 Mix	Site 1 (Teal)	47.3	0.31	-0.04	0.51	31	Magnetite A (tetrahedral) site Fe^{3+} and Maghemite A & B sites Fe^{3+}
	Site 2 (Pink)	42.7	0.57	-0.04	0.70	52	Magnetite B (octahedral) site $Fe^{2.5+}$ (valence averaged)
	Site 3 (Orange)	0.0*	0.91	-0.59	0.58	17	Wüstite ($Fe_{1-x}O$) Fe^{2+} site

Table S2. Mössbauer spectroscopy hyperfine fitting parameters measured at 6 K. Magnetic hyperfine field (B_{hf}), isomer shift (δ), quadrupole splitting (ΔE_q), full-width-at-half-maximum (Γ). Estimated errors are in B_{hf} ±0.5 T, δ±0.03 mm/s, ΔE_q±0.04 mm/s, in Γ ±0.01, and relative area ±3%.

Sample	Fit Site (Spectra Color)	B_{hf} (T)	δ (mm/s)	ΔE_q (mm/s)[1]	Γ (mm/s)[2]	Relative area (%)	Attribution
Fe (II)	Site 1 (Teal)	50.5	0.41	-0.02	0.55	45	Magnetite A (tetrahedral) site Fe^{3+} and Maghemite A & B sites Fe^{3+}
	Site 2 (Pink)	52.6	0.52	0.03	0.52	26	Magnetite B (octahedral) site Fe^{3+}
	Site 3 (Orange)	47.6	1.00	-0.36	1.00	29	Magnetite B-site Fe^{2+} and Wüstite ($Fe_{1-x}O$) Fe^{2+} site
Fe (III)	Site 1 (Teal)	50.0	0.31	0.06	1.50	54	Magnetite A (tetrahedral) site Fe^{3+} and Maghemite A & B sites Fe^{3+}
	Site 2 (Pink)	53.0	0.50	-0.05	1.20	27	Magnetite B (octahedral) site Fe^{3+}
	Site 3 (Purple)	48.5	1.11	0.23	1.51	19	Magnetite B-site Fe^{2+}
1:2 Mix	Site 1 (Teal)	50.6	0.38	-0.04	0.50	46	Magnetite A (tetrahedral) site Fe^{3+} and Maghemite A & B sites Fe^{3+}
	Site 2 (Pink)	52.3	0.56	-0.05	0.53	24	Magnetite B (octahedral) site Fe^{3+}
	Site 3 (Orange)	47.3	1.02	-0.38	0.92	30	Magnetite B-site Fe^{2+} and Wüstite ($Fe_{1-x}O$) Fe^{2+} site